Langmuir
Article
pubs.acs.org/Langmuir

A Smart Supramolecular Hydrogel of N^{α}-(4-*n*-Alkyloxybenzoyl)-L-histidine Exhibiting pH-Modulated Properties

Trilochan Patra, Amrita Pal, and Joykrishna Dey*

Department of Chemistry, Indian Institute of Technology, Kharagpur 721 302, India

Received December 2, 2009. Revised Manuscript Received March 30, 2010

Six L-histidine-based amphiphiles, N^{α}-(4-*n*-alkyloxybenzoyl)-L-histidine of different hydrocarbon chain lengths, were designed, synthesized, and examined for their ability to gelate water. Four of members of this family of amphiphiles were observed to form thermoreversible hydrogels in a wide range of pH at room temperature. The structural variations were characterized by critical gelation concentration, gelation time, gel melting temperature (T_{gs}), rheology, and electron microscopy. Among the amphiphiles, the *n*-octyl derivative showed better gelation ability in the studied pH range. The amphiphiles were found to have T_{gs} higher than body temperature (37 °C) showing their stability. Also, relatively higher yield stress (>1000 Pa) values of the hydrogels show their higher strength. The effective gelator molecules self-assemble into fibrous structures. Scanning electron microscopic picture of the hydrogels revealed large ribbons with right-handed twist. Small-angle XRD and circular dichroism spectroscopy were also employed to characterize the hydrogels. It was observed that $\pi-\pi$ stacking, hydrophobic interaction, amide hydrogen bonding, and solubility factor contribute to the stability and strength of the hydrogels.

Introduction

Hydrogels are a class of soft materials which are prevalent in our daily life. But they continue to attract considerable attention of present-day chemists and biologists in terms of their versatile applications in agricultural, environmental, and medical uses.[1] In particular, hydrogels are of great interest because of their capability to entrap a large number of water molecules per one gelator molecule and exhibiting swelling, which is suitable for their use in biomedical applications and tissue engineering,[1b,2] biosensing,[3a−c] nanotechnology,[3d−f] controlled drug release,[1f,4a−c] gene delivery,[4d−f] and water pollution control.[4g−i] For applications like drug controlled-release systems or bioseparations, hydrogels are required to respond to stimuli such as temperature, pH, and ions. Consequently, during the past 20 years, multistimuli-responsive hydrogels were investigated.[5] But most of these hydrogels are formed by polymers. To date, a wide variety of hydrogels of natural or synthetic polymers have been reported. Because of their superior material properties,[6] polymeric hydrogels were given importance in comparison to low-molecular-weight hydrogelators (LMWHs). However, constrained synthesis, chemical cross-linking, thermosetting nature, toxicity, and slow response to external stimuli[7] limit applications of these high-molecular-weight polymeric gels. The "supramolecular gels" or "physical gels"[1a] of LMWHs, on the other hand, offer various advantages over the conventional polymer gels as gelator molecules are assembled together by noncovalent forces, such as electrostatic, hydrogen-bonding (abbreviated H-bonding, hereafter), dipole−dipole, $\pi-\pi$ stacking, and hydrophobic/van der Waals interactions. For example, one can easily control gel characteristics by changing pH, temperature, and composition of the aqueous solutions. Since the cross-links between fibers are noncovalent in nature, LMWHs exhibit thermoreversibility, rapid response to external stimuli, and bidegradability. It should be noted that for hydrogelation by LMWHs hydrophobic forces are more important.[8]

Examples of small organic molecules (LMWHs) that spontaneously gelate water are very less and often found by accident. But such molecules have drawn considerable attention in the past two decades.[9] The subject has been recently reviewed by Weiss and Terech.[9j] Among these LMWHs, amino acid-based amphiphiles have been paid much attention in recent past because of their biocompatibility and eco-friendly nature.[9h−j,10] As a part of the

*Author for correspondence: Ph 91-3222-283308; Fax 91-3222-255303; e-mail joydey@chem.iitkgp.ernet.in.

(1) (a) Estroff, L. A.; Hamilton, A. D. *Chem. Rev.* **2004**, *104*, 1201. (b) Lee, K. Y.; Mooney, D. J. *Chem. Rev.* **2001**, *101*, 1869. (c) Sangeetha, N. M.; Maitra, U. *Chem. Soc. Rev.* **2005**, *34*, 821. (d) Sannino, A.; Demitri, C.; Madaghiele, M. *Materials* **2009**, *2*, 353–373. (e) Abd El-Rehim, H. A.; Hegazy, E. A.; Abd El-Mohdy, H. L. *J. Appl. Polym. Sci.* **2004**, *93*, 1360. (f) Gupta, P.; Vermani, K.; Garg, S. *Drug Discovery Today* **2002**, *7*, 569. (g) Tiller, J. C. *Angew. Chem., Int. Ed.* **2003**, *42*, 3072.

(2) (a) Yu, L.; Ding, J. *Chem. Soc. Rev.* **2008**, *37*, 1473. (b) Yang, Z.; Xu, K.; Wang, L.; Gu, H.; Wei, H.; Zhang, M.; Xu, B. *Chem. Commun.* **2005**, 4414. (c) Kim, J.; Nayak, S.; Lyon, L. A. *J. Am. Chem. Soc.* **2005**, *127*, 9588. (d) Fedorovich, N. E.; Alblas, J.; Wijn, J. R. D.; Hennink, W. E.; Verbout, A. J.; Dhert, W. J. A. *Tissue Eng.* **2007**, *13*, 1905. (e) Yan, H.; Saiani, A.; Gough, J. E.; Miller, A. F. *Biomacromolecules* **2006**, *7*, 2776.

(3) (a) Liu, H.; Liu, C.; Jiang, L.; Liu, J.; Yang, Q.; Guo, Z.; Cai, X. *Electroanalysis* **2007**, *20*, 170. (b) Bhuniya, S.; Kim, B. H. *Chem. Commun.* **2006**, 1842. (c) Justin, G.; Finley, S.; Abdur Rahman, A. R.; Guiseppi-Elie, A. *Biomed. Microdevices* **2009**, *11*, 103. (d) Kim, J. H.; Lee, T. R. *Langmuir* **2007**, *23*, 6504. (e) Kim, T. H.; Seo, J.; Lee, S. J.; Lee, S. S.; Kim, J.; Jung, J. H. *Chem. Mater.* **2007**, *19*, 5815. (f) Salata, O. V. *J. Nanobiotechnol.* **2007**, *5*, 5.

(4) (a) Vinogradov, S. V. *Curr. Pharm. Des.* **2006**, *12*, 4703. (b) Jo, Y. S.; Gantz, J.; Hubbell, J. A.; Lutolf, M. P. *Soft Matter* **2009**, *5*, 440. (c) Lin, C. C.; Metters, A. T. *Adv. Drug Delivery Rev.* **2006**, *58*, 1379. (d) Cohen, H.; Levy, R. J.; Gao, J.; Fishbein, I.; Kousaev, V.; Sosnowski, S.; Slomkowski, S.; Golomb, G. *Gene Ther.* **2000**, *7*, 1896. (e) Shen, H.; Goldberg, E.; Saltzman, W. M. *J. Controlled Release* **2003**, *86*, 339. (f) Shea, L.; Smiley, E.; Bonadio, J.; Mooney, D. J. *Nat. Biotechnol.* **1999**, *17*, 551. (g) Tang, Q.; Sun, X.; Li, Q.; Wu, J.; Lin, J. *Sci. Technol. Adv. Mater.* **2009**, *10*, 015002 (7 pp). (h) Kofinas, P.; Kioussis, D. R. *Environ. Sci. Technol.* **2003**, *37*, 423. (i) Kiyonaka, S.; Sugiyasu, K.; Shinkai, S.; Hamachi, I. *J. Am. Chem. Soc.* **2002**, *124*, 10954.

(5) (a) Bhattacharya, S.; Eckert, F.; Boyko, V.; Pich, A. *Small* **2007**, *3*, 650. (b) Park, S.; Lee, Y.; Bae, K. H.; Ahn, C. H.; Park, T. G. *Macromol. Rapid Commun.* **2007**, *28*, 1172. (c) Karbarz, M.; Pulka, K.; Misicka, A.; Stojek, Z. *Langmuir* **2006**, *22*, 7843. (d) Shim, W. S.; Yoo, J. S.; Bae, Y. H.; Lee, D. S. *Biomacromolecules* **2005**, *6*, 2930.

(6) (a) Dandu, R.; Cresce, A. V.; Robert Briber, R.; Dowell, P.; Cappello, J.; Ghandehari, H. *Polymer* **2009**, *50*, 366. (b) Dang, J. M.; Leong, K. W. *Adv. Drug Delivery Rev.* **2006**, *58*, 487. (c) Casolaro, M.; Paccagnini, E.; Mendichi, R.; Ito, Y. *Macromolecules* **2005**, *38*, 2460. (d) Lee, K.; Asher, S. A. *J. Am. Chem. Soc.* **2000**, *122*, 9534. (e) Li, Y.; Tang, Y.; Narain, R.; Lewis, A. L.; Armes, S. P. *Langmuir* **2005**, *21*, 9946. (f) Quick, D. J.; Anseth, K. S. *J. Controlled Release* **2004**, *96*, 341. (g) Roy, K.; Wang, D.; Hedley, M. L.; Barman, S. P. *Mol. Ther.* **2003**, *7*, 401–408.

(7) (a) Shah, K. R. In *Polymeric Materials Encyclopedia*; Salamone, J. C., Ed.; CRC Press: Boca Raton, FL, 1996; p 3092. (b) Bhattacharya, S.; Acharya, S. N. G. *Chem. Mater.* **1999**, *11*, 3504.

(8) (a) Israelchivili, J. *Intermolecular and Surface Forces*, 2nd ed.; Academic Press: New York, 1991. (b) Gaspar, L. J. M.; Baskar, G. *J. Mater. Chem.* **2005**, *15*, 5144. (c) Roy, S.; Dasgupta, A.; Das, P. K. *Langmuir* **2007**, *23*, 11769.

Chart 1. Molecular Structures of C_n-OBH Amphiphiles

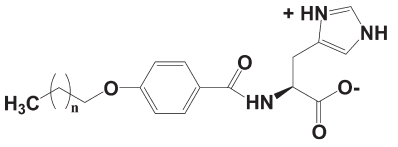

n = 4 (C_6-OBH), 6 (C_8-OBH), 8 (C_{10}-OBH), 10 (C_{12}-OBH)

ongoing research carried out in our laboratory in the direction of self-assembly formation by amino acid-based amphiphiles and their probable use in drug delivery,[9h,9i,11] we have recently shown that *N*-(4-*n*-alkyloxybenzoyl)-L-carnosine amphiphiles act as efficient hydrogelators in a wide pH range.[12] L-Carnosine is a dipeptide containing β-alanine and L-histidine residues. Histidine is considered to be essential in human infants and becomes a nonessential amino acid for the adult. The presence of histidine in protein cause buffering and is a common coordinating ligand in metalloproteins and is a part of catalytic sites in certain enzymes.[13] Monohistidylated cationic amphiphiles have been reported to have remarkable gene transfection properties via the endosome-disrupting characteristics of the histidine functionalities.[14] On the other hand, comicelles of *N*-acyl-L-histidine and various cationic surfactants have been found to be very effective in stereoselective micelle-catalyzed deacylation of long-chain amino acid esters.[15] Antioxidant activity toward lipid peroxidation and excellent emulsifying activity of *N*-acyl-L-histidine have also been reported.[16] In fact, histidine-derived amphiphiles behave as an unusual surfactant because the hydrophilic part contains a carboxylate group and an imidazole side chain, offering the molecule pH-responsive properties.[17] This led us to design, synthesize, and examine gelation abilities of a series of N^{α}-(4-*n*-alkyloxybenzoyl)-L-histidine amphiphiles (C_n-OBH, see Chart 1 for structures) in water. The pH-responsive properties of imidazole ring can make histidine derivative to produce "intelligent gels" or "smart hydrogels".[18] Aggregation behavior of histidine-based amphiphiles has been studied earlier,[17,19] but the gelation ability was not fully explored.[19b,20] The major objectives of this study are (i) to examine gelation abilities of C_n-OBH amphiphiles and (ii) to investigate the effects of environmental factors such as pH and temperature on the gelation process. The hydrogels have been characterized by a number of techniques including electron microscopy, XRD, rheology, and circular dichroism spectroscopy.

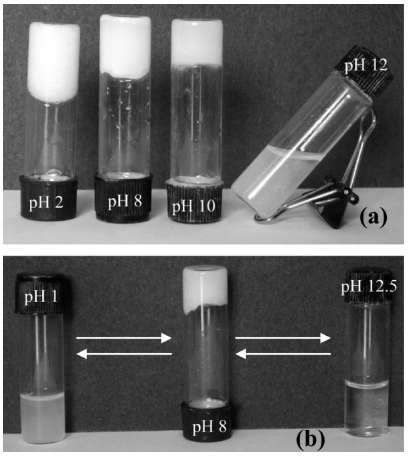

Figure 1. Photographs of vials showing (a) gelation of C_8-OBH at pH 2.0, 8.0, 10.0, and 12.0 in 20 mM phosphate buffer and (b) pH-reversible gelation.

Results and Discussion

Gelation Behavior. The gelation of the amphiphiles C_6-OBH, C_8-OBH, C_{10}-OBH, C_{12}-OBH, C_{14}-OBH, and C_{16}-OBH was tested in different pH of 20 mM phosphate buffer (Figure 1). We found that the C-14 and C-16 analogues remained insoluble in all pH employed, even when strongly heated at 100 °C. Also, the C-6, C-8, C-10, and C-12 derivatives remained insoluble at pH 4 and 5 even when strongly heated in a hot water bath. However, the amphiphiles C_6-OBH, C_8-OBH, C_{10}-OBH, and C_{12}-OBH showed gelation in pH 2 and 7−11.On the other hand, shorter chain length amphiphiles C_6-OBH and C_8-OBH also showed gelation in pH 3 and 6 and pH 6, respectively. The gelation occurred just by one or two alternate heating and cooling cycles. For long chain derivatives C_{10}-OBH and C_{12}-OBH strong heating for longer time was needed for solubilization and gelation of the compound. As can be seen in Figure 1a, the hydrogels are white and opaque, indicating the presence of large aggregates that have sizes comparable to the wavelengths of visible light. The amphiphiles become readily soluble in pH 12.5 buffers at room temperature. Interestingly, we observed that the sol can switch back to the gel form when the pH is adjusted to the range 7−11 or 1−2 in the hot condition and allowed to cool at room temperature (Figure 1b). This indicates that the sol−gel transition is reversible and is an interesting feature of the systems.

Since gelation depends on solubilization in a solvent, it is directly affected by the structure of the compound. This class of compounds, which exist mostly in three different forms cationic, zwitterionic, and anionic (Figure 2), at different pH shows variation in their solubilities and hence gelation. The gel formation of the amphiphiles in water was tested by the "stable to inversion of the test tube" method. The gels formed in all the pH solutions were optically opaque. The gelation behavior of the amphiphiles has been summarized in Table 1. In a given solvent,

(9) (a) Fuhrhop, J.-H.; Boettcher, C. *J. Am. Chem. Soc.* **1990**, *112*, 1768. (b) Oda, R.; Huc, I.; Candau, S. J. *Angew. Chem., Int. Ed. Engl.* **1998**, *37*, 2689. (c) Menger, F. M.; Caran, K. L. *J. Am. Chem. Soc.* **2000**, *122*, 11679. (d) Marmillon, C.; Gauffre, F.; Gulik-Krzywicki, T.; Loup, C.; Caminade, A.-M.; Rump, E. *Angew. Chem., Int. Ed.* **2001**, *40*, 2626. (e) Iwaura, R.; Yoshida, K.; Masuda, M.; Yase, K.; Shimizu, T. *Chem. Mater.* **2002**, *14*, 3047. (f) Friggeri, A.; Feringa, B. L.; Esch, J. V. *J. Controlled Release* **2004**, *97*, 241. (g) Zhou, S.-L.; Matsumoto, S.; Tian, H.-D.; Yamane, H.; Ojida, A.; Kiyonaka, S.; Hamachi, I. *Chem.—Eur. J.* **2005**, *11*, 1130. (h) Khatua, D.; Maiti, R.; Dey, J. *Chem. Commun.* **2006**, 4903. (i) Ghosh, A.; Dey, J. *Langmuir* **2009**, *25*, 8466. (j) *Molecular Gels: Materials with Self-Assembled Fibrillar Networks*; Weiss, R. G., Terech, P., Eds.; Springer: New York, 2006.

(10) (a) Kaneko, D.; Olsson, U.; Sakamoto, K. *Langmuir* **2002**, *18*, 4699. (b) Suzuki, M.; Owa, S.; Yumoto, M.; Kimura, M.; Shirai, H.; Hanabusa, K. *Tetrahedron Lett.* **2004**, *28*, 5399. (c) Das, D.; Dasgupta, A.; Roy, S.; Mitra, R. N.; Debnath, S.; Das, P. K. *Chem.—Eur. J.* **2006**, *12*, 5068. (d) Pal, A.; Ghosh, Y. K.; Bhattacharya, S. *Tetrahedron* **2007**, *63*, 7334. (e) Shome, A.; Debnath, S.; Das, P. K. *Langmuir* **2008**, *24*, 4280.

(11) Khatua, D.; Dey, J. *Langmuir* **2005**, *21*, 109.

(12) Pal, A.; Shrivastava, S.; Dey, J. *Chem. Commun.* **2009**, 6997–6999.

(13) (a) Bertini, I.; Scozzafava, A. In *Metal Ions in Biological Systems*; Sigel, H., Ed.; Marcel Dekker: New York, 1981; Vol. *12*, pp 31−74. (b) Casolaro, M.; Chelli, M.; Ginanneschi, M.; Laschi, F.; Messori, L.; Muniz-Miranda, M.; Papini, A. M.; Kowalik-Jankowska, T.; Kozlowsky, H. *J. Inorg. Biochem.* **2002**, *89*, 181. (c) Kowalik-Jankowska, T.; Jasionowski, M.; Lankiewicz, L. *J. Inorg. Biochem.* **1999**, *76*, 63. (d) Bonomo, R.; Conte, E.; Impellizzeri, G.; Pappalardo, G.; Purrello, R.; Rizzarelli, E. *J. Chem. Soc., Dalton Trans.* **1996**, 3093.

(14) Kumar, V. V.; Pichon, C.; Refregiers, M.; Guerin, B.; Midoux, P.; Chaudhuri, A. *Gene Ther.* **2003**, *10*, 1206.

(15) Ohkubo, K.; Sugahara, K.; Ohta, H.; Tokuda, K.; Ueoka, R. *Bull. Chem. Soc. Jpn.* **1981**, *54*, 576.

(16) Murase, H.; Nagao, A.; Terao, J. *J. Agric. Food Chem.* **1993**, *41*, 1601.

(17) Smith, G. D.; Barden, R. E. *Chem. Phys. Lipids* **1975**, *14*, 1.

(18) Dagani, R. *Chem. Eng. News* **1997**, *75*, 26.

(19) (a) Yamada, K.; Shosenji, H.; Ihara, H. *Chem. Lett.* **1979**, 491. (b) Ragunath, K. G.; Bhattacharya, S. *Chem. Phys. Lipids* **1995**, *77*, 13. (c) Varka, E.-M. A.; Heli, M. G.; Argyropoulou, E. C.; Pegiadou, S. A. *Chem.—Eur. J.* **2006**, *12*, 8305.

(20) (a) Casolaro, M.; Bottari, S.; Cappelli, A.; Mendichi, R.; Ito, Y. *Biomacromolecules* **2004**, *5*, 1325. (b) Casolaro, M.; Bottari, S.; Ito, Y. *Biomacromolecules* **2006**, *7*, 1439.

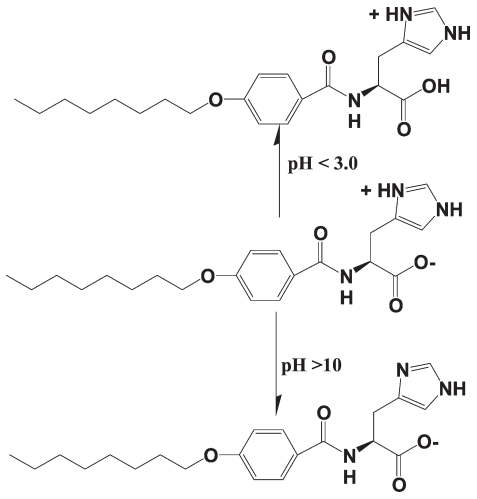

Figure 2. Proton transfer forms of C_8-OBH.

Table 1. Results of Gelation Test at Various pH in 20 mM Phosphate Buffer[a]

	CGC (mg/mL)			
pH	C_6-OBH	C_8-OBH	C_{10}-OBH	C_{12}-OBH
2.0	2.5 (328)	2.0 (347)	2.0 (339)	2.3 (337)
3.0	4.5	I	I	I
4.0	I	I	I	I
5.0	I	I	I	I
6.0	5.4	2.1	I	I
7.0	5.2	1.9	2.1	2.1
8.0	2.8 (321)	1.5 (341)	1.5 (336)	1.9 (333)
9.0	2.9	2.2	3.1	3.2
10.0	3.1	2.5	3.2	3.5
11.0	5.0	4.8	8.9	15.1
12.0	S	S	S	S

[a] Values refer to the critical gelation concentration (CGC, mg/mL) necessary for gelation at 25 °C; S: solution, I: insoluble. Values in the parentheses represent T_{gs} in K.

gelation occurred when a critical concentration, called critical gelation concentration (CGC), of the gelator is reached. It is defined as minimum amount of gelator that can gelate maximum volume of solvent. The CGC values (mg/mL) necessary for gelation at various pH for the amphiphiles are shown in Table 1. It is important to note that the CGC values are less than 10 mg/mL, which corresponds to gelation capacity of less than 1% (w/v). In other words, as many as 2000 mol of water molecules is trapped by 1 mol of gelator molecules. This means that the amphiphiles are among the most efficient amino acid-based amphiphilic hydrogelators. At room temperature and at gelator concentration close to CGC, it took 10−12 h for the gelation to take place. However, with the increase of the amount and chain length of the gelator, the gelation kinetics becomes faster. The hydrogels remained unchanged for more than 2 months when preserved under constant conditions at low temperature (20 °C). Interestingly, the hydrogels having gelator concentration around the CGC value shrunk by expelling water after a week or so when stored at temperature greater than 20 °C.

Influence of pH and Hydrocarbon Chain Length on Gelation. Since the compound exists in different forms (see Figure 2) at different pH, the solution pH has a definite role in gelation of amphiphiles. Since at pH > 12 the gelator molecule exists in the anionic form, the gelator−gelator interaction is weakened due to ionic repulsion and thus becomes more soluble in water. This means less number of gelator molecules in the aggregate and hence formation of small size aggregates. On the other hand, in the pH range 6−10, the molecules remain mostly in the zwitterionic form which means less aqueous solubility and increase of gelator−gelator hydrophobic interaction. These result in a formation of large aggregates that subsequently upon physical entanglement produce 3-D network structure. The CGC value can be used to understand the influence of solution pH on gelation. It was found that for a particular amphiphile the CGC value is lowest at pH 8 and highest at pH 11.

It should be noted that at a particular pH the lowest CGC value was obtained with C_8-OBH. This suggests that solubilization, i.e., hydrophilic−lipophilic balance (HLB), in an amphiphile is responsible for hydrogelation. In the case of C_6-OBH, the smaller hydrocarbon tail increases the solubility and weakens gelator−gelator interaction, whereas with C_{10}-OBH and C_{12}-OBH long chain hindered the solubility at all pH, resulting in high CGC. However, C_8-OBH was found to have optimum HLB for better gelation in all the pH solutions as indicated by the lower CGC values. So an optimum solubility of the amphiphiles is required for gelation to occur. Such HLB is well-known in the molecular assembly of biological membranes. For higher alkyl chain lengths, the high CGC value may also be explained by the partial tilt or bending of the long hydrocarbon chain, which weakens the gelator−gelator directional (e.g., H-bonding) forces, thereby increasing the CGC value.

Microscopic Observations. As discussed earlier, the gelators form large self-assembled aggregates in water. To obtain visual images of the gel aggregates of the amphiphiles at a given pH, the morphology of the dry hydrogels of C_6-OBH, C_8-OBH, C_{10}-OBH, and C_{12}-OBH was investigated by the FE-SEM technique. The morphology shows fibrous network structure which confirms gelation by these amphiphiles. In a magnified view (Figure 3) we found these fibers are made up of bundle of helical ribbons. As the chirality of the gelators is directly translated into the chirality of the gel fiber, so the chirality of the microstructures can be clearly visualized showing the right handed helical ribbons for all the amphiphiles at both lower and higher pHs. The lengths of the fibrous bundles are of the order of several micrometers and some time visible to the naked eye in concentrated solution, and their widths are ranging from 200 nm to 2 μm. It was found that the ribbons are either cross-linked or running parallel to each other.

Influence of Chirality. The chirality of a gelator molecule often plays a significant role in controlling and mediating the self-assembly of the gelator.[21] In fact, many gelator molecules include chiral centers and are considered to be very important for the gelation process. The gelling ability of a compound of pure enantiomer is always found to be better than the racemic form. The chirality is often translated through formation of chiral aggregates. Many chiral *N*-acyl amino acid amphiphiles are known to form helical aggregates in water.[22−24] Recently, Weiss

(21) Brizard, A.; Oda, R.; Huc, I. *Top. Curr. Chem.* **2005**, *256*, 167.
(22) (a) Du, X.; Hlady, V. *J. Phys. Chem. B* **2002**, *106*, 7295. (b) Du, X.; Liang, Y. *J. Phys. Chem. B* **2001**, *105*, 6092. (c) Du, X.; Liang, Y. *J. Phys. Chem. B* **2000**, *104*, 10047. (d) Miyagishi, S.; Takeuchi, N.; Asakawa, T.; Itoh, M. *Colloids Surf., A* **2002**, *197*, 125.
(23) (a) Zhang, Y.-J.; Jin, M.; Lu, R.; Song, Y.; Jiang, L.; Zhao, Y. *J. Phys. Chem. B* **2002**, *106*, 1960. (b) Boettcher, C.; Schade, B.; Fuhrhop, J.-H. *Langmuir* **2001**, *17*, 873. (c) Vollhardt, D.; Gehlert, U. *J. Phys. Chem. B* **2002**, *106*, 4419. (d) Kawasaki, H.; Souda, M.; Tanaka, S.; Nemoto, N.; Karlsson, G.; Almgren, M.; Maeda, H. *J. Phys. Chem. B* **2002**, *106*, 1524. (e) Yeoh, K. W.; Chew, C. H.; Gan, L. M.; Koh, L. L.; Teo, H. H. *J. Macromol. Sci., Part A* **1989**, *26*, 663.
(24) (a) Roy, S.; Dey, J. *Langmuir* **2005**, *21*, 10362. (b) Dey, J.; Roy, S. *Langmuir* **2003**, *19*, 9625. (c) Song, J.; Cheng, Q.; Kopta, S.; Stevens, R. *J. Am. Chem. Soc.* **2001**, *123*, 3205. (d) Bhattacharyya, S.; Krishnan-Ghosh, Y. *J. Chem. Soc., Chem. Commun.* **2001**, 185. (e) Luo, X.; Liu, B.; Liang, Y. *Chem. Commun.* **2001**, 1556. (f) Shinitzky, M.; Haimovitz, R. *J. Am. Chem. Soc.* **1993**, *115*, 12545.

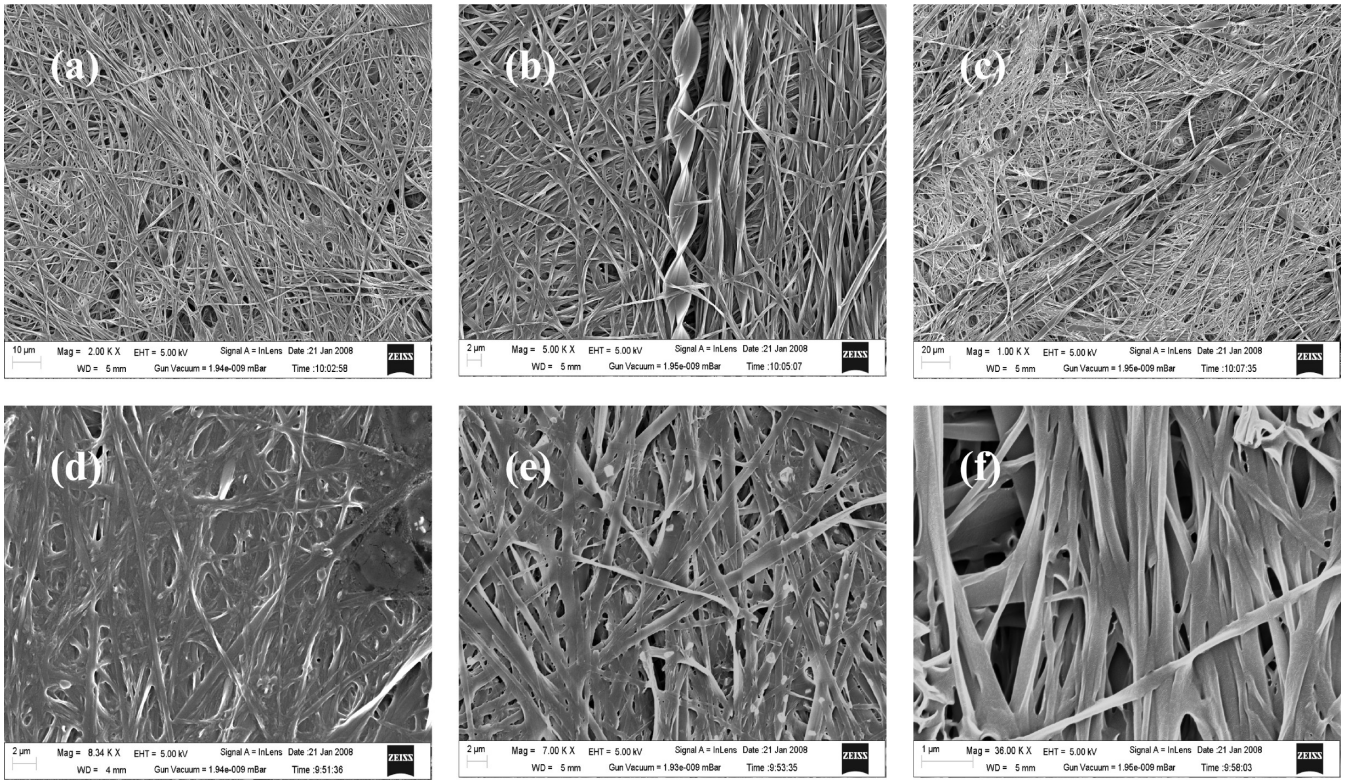

Figure 3. FE-SEM images of the dry hydrogels of C_6-OBH, at pH 2.0 (a), pH 8.0 (b), and pH 10.0 (c) and of C_8-OBH at pH 2.0 (d), pH 8.0 (e), and pH 10.0 (f).

and co-workers have studied the kinetics of self-assembled fibrillar network formation of *p*-nitrobenzyl arjunolate in mixed organic solvent by CD spectroscopy.[25] The chirality-induced helicity in molecular self-assembly of C_8-OBH is clearly observed in the micrograph b of Figure 3. Homochiral interactions between histidine headgroups of the gelators perhaps facilitate one-dimensional (1-D) growth of the fibrous aggregates, the physical entanglement of which leads to the 3-D network structures. The homochiral interaction among chiral amphiphiles should lead to the formation of 1-D helical fibers, which can be further confirmed by the characteristic circular dichroism (CD) spectrum.[26] Since the hydrogel formed by C_8-OBH is optically opaque, the aqueous solution of the amphiphile was analyzed for chiral organization by CD spectroscopy. Figure 4 shows the CD spectra of C_8-OBH in methanol and in pH 8 and 12 having concentration much less than CGC. The negative band in the wavelength range 215−240 nm of the CD spectrum in pH 8 solution supports the existence of helical aggregates. The formation of helical aggregates was also observed with the structurally similar amphiphile, sodium *N*-[4-*n*-dodecyloxybenzoyl]-L-valinate.[27] Since even dilute solution of C_8-OBH is not transparent, we could not measure the CD spectrum in pH 2.0 solution.

X-ray Diffraction Studies. The XRD patterns of the air-dried gel cast film of C_8-OBH in pH 2.0, 8, and 10.0 as representative example have been depicted in Figure 5. From the peak positions (2θ values) corresponding planes and interplanar distances (d) were calculated using Bragg's equation. The hydrogel of C_8-OBH exhibits periodical diffraction peaks with their positions approximately at a ratio of 1:2:3:4, which suggests an ordered lamellar phase. This is consistent with the FESEM images

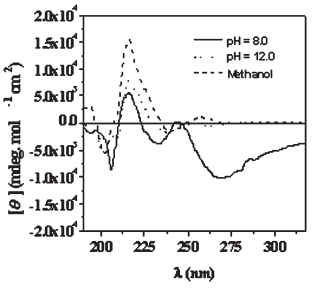

Figure 4. Circular dichroism spectra of 2.0 mM C_8-OBH in phosphate buffers of pH 8 and 12 and in methanol.

shown in Figure 3. These peaks are due to the length of a repeat unit along the long axis of the molecule. The XRD data suggest that in all the three pH the hydrogels have similar morphology and are crystalline in nature.

Viscoselastic Behavior. During the gelation test, it was observed that the hydrogels in all the pH-containing gelators corresponding to the CGC value partially broke down and part of the trapped water was expelled out, even upon gentle shaking of the vial. This indicated that the hydrogels are less rigid. The rheological properties of the hydrogels of C_8-OBH as a representative example were studied at three different pH values. The mechanical strength of a gel which is measured by the storage modulus (G') and loss modulus (G'') is dependent on gelator concentration. We measured these quantities as a function of applied stress (σ) and frequency on the hydrogels of C_8-OBH in pH 2, 8, and 10 that contained gelator of ca. 5 times its CGC value. Figure 6 shows the variation of G' and G'' with strain frequency. It is seen that in all the pH both G' and G'' are almost independent of frequency which is characteristic of gel structure. Also at any given frequency, the G' much higher than G'',

(25) Bag, B. G.; Dinda, S. K.; Dey, P. P.; Mallia, A.; Weiss, R. G. *Langmuir* **2009**, *22*, 8663.
(26) Helfrich, W.; Prost, J. *Phys. Rev. A* **1988**, *38*, 3065.
(27) Mohanty, A.; Dey, J. *Langmuir* **2004**, *20*, 8452.

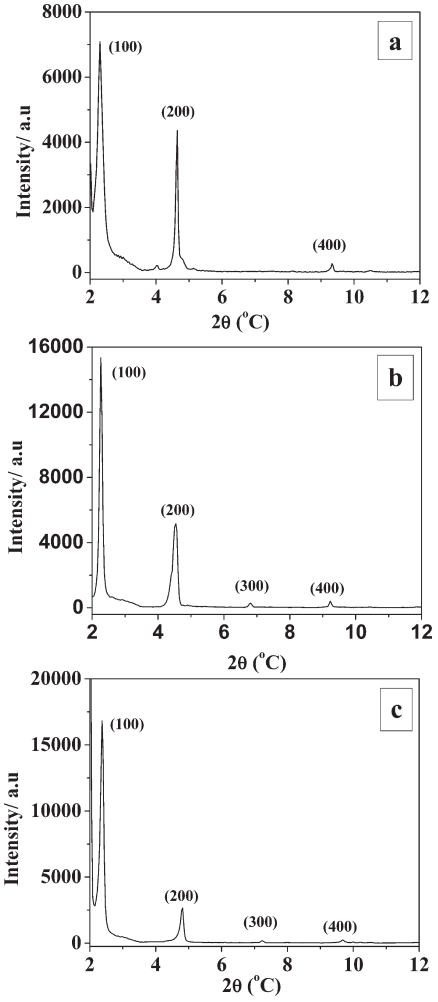

Figure 5. X-ray diffraction pattern of hydrogel film of C_8-OBH at (a) pH 2, (b) pH 8, and (c) pH 10.

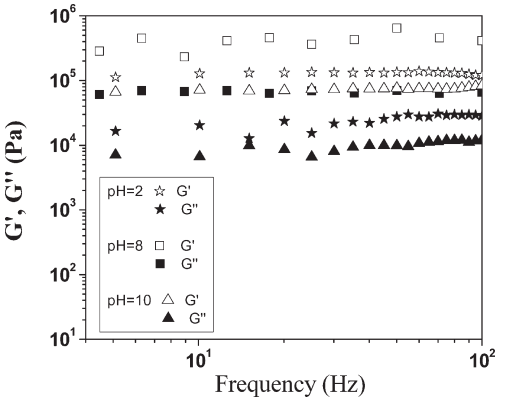

Figure 6. Variation of storage modulus (G') and loss modulus (G'') with frequency (f) of hydrogel C_8-OBH in pH 2.0, 8.0, and 10.0 at 298 K.

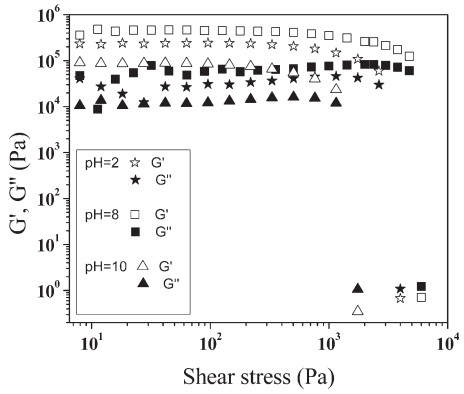

Figure 7. Variation of storage modulus (G') and loss modulus (G'') with shear stress (σ) of hydrogel C_8-OBH in pH 2.0, 8.0, and 10.0 at 298 K.

indicating more elastic nature of the gels like solids. The difference between G' and G'' can be taken as an indicator of the rigidity or stability of a gel. The ($G' - G''$) values were ca. 98 220, 342 308, and 61 921 Pa for the hydrogels in pH 2, 8, and 10, respectively. This means that the hydrogel in pH 8 is more firm and rigid than hydrogel in pH 2 which in turn more firm than the gel in pH 10. Figure 7 shows the plots of G' and G'' versus applied stress (σ) at a constant frequency of 1 Hz. It can be observed that above a critical stress value both G' and G'' abruptly fall to a very low value, indicating flow of the hydrogel. This critical stress value is referred to as yield stress (σ_y). The σ_y values at pH 2, 8, and 10 as obtained from the breakpoint of the respective plot are respectively, 2662, 4830, and 1190 Pa. The σ_y values are quite large, suggesting high mechanical strength of the hydrogels. However, the hydrogel in pH 8 has the highest yield stress value that decreases both upon decrease and increase of the acidity of water. Such modulation in viscoelastic properties with pH is an interesting feature of the system and has significant value as far as drug release is concerned. The change in viscoelastic properties can be attributed to the variation of supramolecular interactions and hence 3-D network structure in the hydrogel at different pH.

Thermal Stability of the Hydrogels. It is well established that gel formation is strongly dependent on the gelator concentration and temperature. Since higher gelator concentration promotes growth self-assemblies, gelation is favored. On the other hand, higher temperature dismantles self-assemblies and thus disfavors gel formation. We have determined the gel melting temperature that is gel-to-sol transition temperature (T_{gs}) of the hydrogels (Table 1) at different pH, keeping the amount of gelator (15 mM) fixed. The gel melting temperature was determined by placing the screw-cap glass vials containing gels in a temperature-controlled water bath and visually observing the flow upon tilt for every degree rise in temperature. Although the gel structure was found to melt upon heating, the gelation of the solution took place upon cooling to room temperature. That is, the gels are thermoreversible. All the hydrogels have T_{gs} above 37 °C. Thus, the hydrogels formed by different amphiphiles at various pH were found to be thermally quite stable. The variation of T_{gs} with the number of carbon atoms (N_C) of the hydrocarbon chain of the gelators has been shown by the bar graph in Figure 8a. It has been found that for any gelator T_{gs} is less in pH 2 than in pH 8. This is consistent with the yield stress values. Also, at any given pH, T_{gs} was found to be highest for C_8-OBH. The gel melting temperature of C_8-OBH was also measured at various concentrations in pH 8 as well as in pH 2. Figure 8b shows the plots of T_{gs} versus [C_8-OBH]. It is observed that the T_{gs} value increases linearly with [C_8-OBH] in the concentration range studied.

The T_{gs} value is consistent with the lower CGC value of C_8-OBH. For C_{10}-OBH and C_{12}-OBH, perhaps, lower solubility or partial folding of the hydrocarbon chain or both hinder growth of self-assemblies. This means formation of short fibers which results in less entanglement of the fibers and hence higher CGC value and lower yield stress and T_{gs} values. The increase of concentration, on the other hand, facilitates growth of the fibers, thereby causing more entanglement. This is reflected by the increase of T_{gs} value.

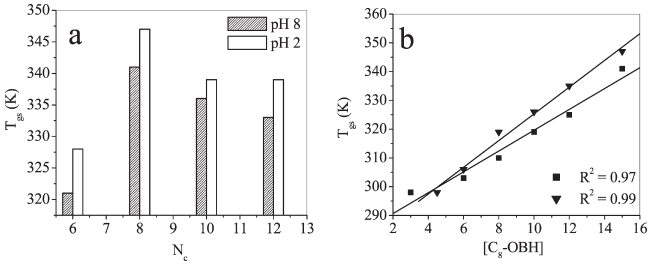

Figure 8. (a) Variation of gel melting temperature (T_{gs}) with hydrocarbon chain length (N_C) at pH 2 and pH 8. (b) Plot of gel melting temperature (T_{gs}) versus [C_8-OBH] at pH 2 (▲) and pH 8 (■).

Driving Force for Aggregate Formation. It is well-known that lipophilic (hydrophobic) interactions between gelator molecules in strongly H-bonding and polar solvents provide a major contribution to the overall stabilization of the assemblies while H-bonding usually gives a dominant contribution in lipophilic solvents.[28] The role of amide H-bonding in the self-assembly formation in water by *N*-acyl amino acid amphiphiles has already been reported in the literature.[23,24] In fact, we have already demonstrated intermolecular H-bonding in the formation of bilayer self-assemblies by a structurally similar amphiphile, sodium *N*-[4-*n*-dodecyloxybenzoyl]-L-valinate.[27] Further, to examine the possible role of lipophilic interactions, including $\pi-\pi$ stacking in aggregate formation by C_8-OBH, we have measured variable temperature (298−343 K) ^{1}H NMR spectra of its hydrogel prepared in D_2O solvent. The representative ^{1}H NMR spectra of C_8-OBH (ca. 0.5% w/v, in D_2O) at temperatures 298 and 343 K have been shown in Figure S1 of the Supporting Information. Usually the signals of gelator molecules assembled in the 3-D gel network are not observed due to long correlation times. Thus, the observed gelator signals are due to the smaller assemblies dissolved in the entrapped D_2O solvent. The $\pi-\pi$ stacking interaction can be confirmed from the change in chemical shift (δ) of the aromatic protons. The signals of the phenyl protons (Ph*H*) of C_8-OBH molecule have merged into one broad band even at elevated temperatures, confirming the assembled state. The signals of imidazole ring protons (Imz*H*), however, are well separated. The δ_H values of both types of protons are observed to shift toward downfield positions linearly (Figure 9) with the increase of temperature. The increase of δ_H value with the increase of temperature suggests a change in the microenvironment of amphiphiles due to loss of H-bonding and $\pi-\pi$ stacking interactions at higher temperatures. The necessity of $\pi-\pi$ stacking is also confirmed by the failure of hydrogel formation by the structurally similar amphiphile, N^{α}-dodecanoyl-L-histidine (L-C_{12}His), which does not have a phenyl group in the hydrocarbon chain. Thus, within the bilayer leaflet, the amphiphiles are connected by intermolecular H-bonds to form H-bond network to develop the superstructures in which the aromatic rings are stacked on top of each other. The detailed microstructural characterization of the hydrogels by spectroscopic and microscopic studies as described above shows that a precise balance between hydrophilicity and hydrophobicity is the key factor in this self-assembling process, which involves intermolecular H-bonding and hydrophobic interactions.

Drug Entrapment and Release Studies. The water-immobilizing ability and the hydrophobic domains in the bilayer aggregates make these hydrogels potential drug carriers. In order

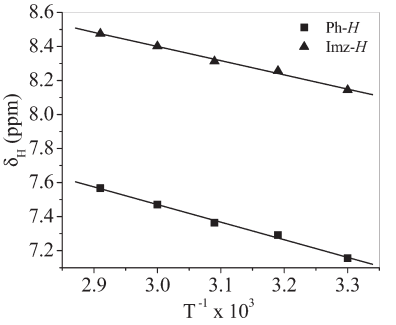

Figure 9. Temperature-dependent chemical shift (δ_H in ppm) of imidazole (Imz) proton (■) and phenyl proton (▲) in 10 mM C_8-OBH gel in 20 mM phosphate buffer of pH 8.

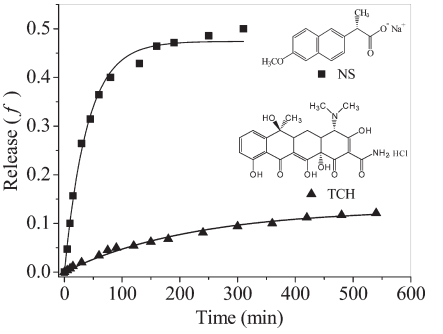

Figure 10. Time-dependent release (*f*) of NS (■) and TCH (▲) in 20 mM phosphate buffer (pH 6) from 8 mM C_8-OBH gel in 20 mM phosphate buffer of pH 8, containing 5×10^{-5} M drug each.

to demonstrate the potential application of the hydrogel of C_8-OBH in drug delivery, we describe the entrapment and release of two small drug molecules: naproxen sodium salt (NS) and tetracycline hydrochloride (TCH). NS is an anti-inflammatory drug, while TCH has antimicrobial activity. TCH was chosen since it can interact with the gelator not only via van der Waals interactions and H-bonding but also more strongly with the carboxylate group of the gelator since it possesses an ammonium group. Consequently, it may be retained within the hydrogel to a greater extent than NS which can interact with the gelator only via weaker van der Waals interactions. Further, both molecules are fairly soluble in water (pH 8) and UV-active, making their release from the hydrogel easy to follow by spectrophotometry.

Thus, 8 mM of C_8-OBH in 1.0 mL of phosphate buffer containing 5×10^{-5} M NS (or TCH) was dispersed in an ultrasonic bath for 5 min followed by three heating−cooling cycles. The mixture was then transferred into a quartz cuvette (1 cm^2) and left at room temperature for gelation to occur. Although the homogeneous mixture turned into gel within a few minutes, it was allowed to stand for equilibration for 1 h at room temperature, after which 2 mL of 20 mM phosphate buffer (pH 6.0) was carefully added on top of the hydrogel with the help of a micropipet. Absorbance of the solution on top of the gel phase was measured at 330 nm (or 360 nm for TCH) at different time intervals. The amount released at any time was calculated as fraction of the total amount dissolved in the gel phase. Assuming that the release of the drug from the gel over time follows first-order kinetics, the data sets were fitted to eq 1:

$$f = 1 - e^{-kt} \quad (1)$$

where *f* is the fraction of NS (or TCH) at time *t* in the solution and *k* is the first-order rate constant. A reasonably good fit can be

(28) Zweep, N.; Hopkinson, A.; Meetsma, A.; Browne, W. R.; Feringa, B. L.; van Esch, J. H. *Langmuir* **2009**, *25*, 8802.

observed in Figure 10 for both the drug molecules. The values of k for NS and TCH were found to be 4.2×10^{-4} and 7.5×10^{-5} s^{-1}, respectively. Thus, the release rate of the entrapped material from the hydrogel of C_8-OBH is observed to be relatively slow for both drug molecules. However, as expected, the release rate of TCH is 10 times slower than that of NS. It is observed that at pH 6 only about 50% and 10% of the entrapped NS and TCH, respectively, were observed to be released within 6 h. It should be noted that no change in the gel phase occurred during the release process. Therefore, it can be concluded that the release of entrapped drug was entirely due to diffusion.

Conclusions

In summary, a family of low-molecular-weight L-histidine-derived hydrogelators (C_n-OBH) that exhibit efficient gelation capability have been synthesized. Among these C_8-OBH acts as an efficient gelator in pH 8.0; the hydrogel of C_8-OBH was found to have the highest thermal and mechanical stability. The pH-dependent reversibly modulated gelation properties of the thermoreversible hydrogels have been reported. Indeed, reversible switching between gel and sol (or precipitate) could be easily controlled by changing pH. The pH dependence of CGC and gel melting temperature T_{gs} suggests that gelation is driven by hydrophobic, hydrogen-bonding, and $\pi-\pi$ stacking interactions. The presence of protons changes supramolecular interactions by forming and breaking intermolecular hydrogen bonds, which controls the degree of branching and interfacial tension in the 3-D hydrogel network. The gelator molecules self-assemble to form 1-D bilayer structures (ribbons) of high aspect ratio in all pH. The chirality of the gelator molecules is translated through formation of chiral aggregates, such as twisted ribbons as manifested by the characteristic CD spectrum and SEM pictures. The ability to form hydrogels by N^{α}-(4-n-alkyloxybenzoyl)-L-histidine amphiphiles has demonstrated that for the pH-dependent hydrogel formation by N-(4-n-alkyloxybenzoyl)-L-carnosine amphiphiles the β-alanine residue of L-carnosine has no significant role. The hydrogels of the L-histidine amphiphiles have high yield stress showing good mechanical strength and exhibit pH-responsive viscoelastic properties. The present study generated a new type of hydrogel and showed a facile route for modulating mechanical properties of supramolecular hydrogels. The gel melting temperature, T_{gs} (concentration-dependent), was observed to be much higher than body temperature (37 °C). Slow release of the anti-inflammatory drug naproxen and antimicrobial drug tetracycline shows that the hydrogel may find applications in transdermal drug delivery. Further work in this direction is currently underway in this laboratory.

Experimental Section

Materials. 4-Hydroxybenzoic acid, 1-bromododecane, 1-bromodecane, 1-bromooctane, anhydrous potassium carbonate, sodium bicarbonate, N-hydroxysuccinimide (NHS), 1,3-dicyclohexylcarbodiimide (DCC), L-histidine, sodium hydrogen carbonate, sodium dihydrogen phosphate, disodium hydrogen phosphate, and sodium hydroxide were purchased from SRL, Mumbai, India, and were used without further purification. Hexyloxybenzoyl chloride was obtained from Aldrich. All the organic solvents were of highest purity commercially available and were dried and distilled fresh before use. Milli-Q water was used for the preparation of buffers. All the surfactants employed in this study were synthesized in the laboratory as described below.

(29) (a) Mohanty, A.; Dey, J. *J. Chem. Soc., Chem. Commun.* **2003**, 1348. (b) Mohanty, A.; Dey, J. *Langmuir* **2007**, *23*, 1033.

Synthesis of Amphiphiles. N^{α}-[4-n-Alkyloxybenzoyl]-L-histidine amphiphiles (C_8-OBH, C_{10}-OBH, and C_{12}-OBH) were synthesized following a procedure described elsewhere.[29] The compounds were purified by recrystallization from acetone−water or ethanol−water mixture. For N^{α}-[4-n-hexyloxybenzoyl]-L-histidine (C_6-OBH), however, L-histidine was directly reacted with hexyloxybenzoyl chloride in the THF/H_2O mixture in the presence of triethylamine (pH 8−9). Chemical identification of all the compounds was performed by use of ^{1}H NMR and FT-IR spectroscopy. The details of chemical identification are available in the Supporting Information.

Methods and Instrumentation. The melting point of solid compounds was measured using the Instind (Kolkata) melting point apparatus with open capillaries. The measurements of optical rotations were performed with a JASCO (model P-1020) digital polarimeter. The FT-IR spectra were measured with a Perkin-Elmer (model Spectrum Rx I) spectrometer. The ^{1}H NMR spectra were recorded on an AVANCE DAX-400 (Bruker, Sweden) 400 MHz NMR spectrometer in CD_3OD or D_2O/NaOD solvent with CH_3CN as a standard. The circular dichroism (CD) spectra were measured with a JASCO J-810 spectropolarimeter using a quartz cell with a path length of 1.0 mm. The kinetics of drug release was studied by use of a Shimadzu (UV-2450) UV−vis spectrophotometer. All measurements were done at 298 K unless otherwise mentioned.

Gelation was studied by dissolving 5 mg of solid gelator in a screw-cap vial in requisite volume of 20 mM phosphate buffer by heating in a hot water bath (~70 °C) and subsequently allowed to cool at 25 °C in a temperature-controlled water bath. Resistance of the mixture to flow under gravity on inversion of the vial indicated gel formation. Melting temperature of the hydrogels was determined by inverted-tube experiment in which the screw-cap vial containing the gel was put in a temperature-controlled water bath (JULABO, model F12). The temperature of the bath was gradually increased at a rate of 1 deg/min, and the temperature was noted where the gelated mass started to flow on tilting of the vial. Each experiment was repeated at least twice. The melting temperature did not vary more than ±1 °C.

For electron micrographs, the hot sample solution was placed on the aluminum or copper foil, allowed to cool, and air-dried at room temperature. The gel cast films were further dried in desiccators for 24 h. A layer of gold was sputtered on top to make conducting surface, and finally the specimen was transferred into the field emission scanning electron microscope (FESEM, Zeiss, Supra-40) operating at 5−10 kV to get the micrograph.

The XRD spectra were taken at room temperature for all air-dried hydrogel samples prepared on a glass slide. The experiment was performed on a Pan analytica X' Pert pro X-ray diffractometer using Cu target (Cu Kα) and Ni filter at a scanning rate of 0.001 s^{-1} between 2° and 12°, operating at a voltage of 40 kV and current 30 mA.

For rheology measurements were performed on a Bohlin RS D-100 (Malvern, UK) rheometer using parallel-plate (PP-20) geometry. The gap between the cone and plate was fixed at 300 μm. The hydrogel was placed on the rheometer, and a stress-amplitude sweep experiment was performed at a constant oscillation frequency of 1.0 Hz at 25 °C.

Acknowledgment. Financial support (Grant SR/S1/PC-18/2005) from Department of Science and Technology, New Delhi, is duly acknowledged. T.P. thanks CSIR, India, for a research fellowship. We thank Dr. Dhara of the School of Medical Science and Technology, IIT, Kharagpur, for assistance with the rheological measurements.

Supporting Information Available: Details of chemical identification of the amphiphiles including spectral data and ^{1}H NMR spectra at different temperatures. This material is available free of charge via Internet at http://pubs.acs.org.